CellPress

Molecular Cell
Article

SWR1 and INO80 Chromatin Remodelers Contribute to DNA Double-Strand Break Perinuclear Anchorage Site Choice

Chihiro Horigome,[1] Yukako Oma,[2] Tatsunori Konishi,[2] Roger Schmid,[1,3] Isabella Marcomini,[1,4] Michael H. Hauer,[1,4] Vincent Dion,[1,5] Masahiko Harata,[2] and Susan M. Gasser[1,4,*]

[1]Friedrich Miescher Institute for Biomedical Research, Maulbeerstrasse 66, 4058 Basel, Switzerland
[2]Laboratory of Molecular Biology, Tohoku University, Tsutsumidori-Amamiyamachi 1-1, Aoba-ku, Sendai 981-8555, Japan
[3]Institute of Plant Biology, University of Zurich, Zollikerstrasse 107, 8008 Zurich, Switzerland
[4]University of Basel, Faculty of Natural Sciences, 4056 Basel, Switzerland
[5]Present address: Center for Integrative Genomics, University of Lausanne, 1015 Lausanne, Switzerland
*Correspondence: susan.gasser@fmi.ch
http://dx.doi.org/10.1016/j.molcel.2014.06.027

SUMMARY

Persistent DNA double-strand breaks (DSBs) are recruited to the nuclear periphery in budding yeast. Both the Nup84 pore subcomplex and Mps3, an inner nuclear membrane (INM) SUN domain protein, have been implicated in DSB binding. It was unclear what, if anything, distinguishes the two potential sites of repair. Here, we characterize and distinguish the two binding sites. First, DSB-pore interaction occurs independently of cell-cycle phase and requires neither the chromatin remodeler INO80 nor recombinase Rad51 activity. In contrast, Mps3 binding is S and G2 phase specific and requires both factors. SWR1-dependent incorporation of Htz1 (H2A.Z) is necessary for break relocation to either site in both G1- and S-phase cells. Importantly, functional assays indicate that mutations in the two sites have additive repair defects, arguing that the two perinuclear anchorage sites define distinct survival pathways.

INTRODUCTION

Improperly repaired DNA double-strand breaks (DSBs) can lead to genomic rearrangements and loss of genetic information (Jackson and Bartek, 2009), making them one of the most hazardous forms of genomic damage. DSBs arise both from exogenous agents, such as γ irradiation or chemical insult, and from endogenous events, such as replication fork collapse (Pfeiffer et al., 2000).

DSB repair is generally achieved by two conserved mechanisms: nonhomologous end-joining (NHEJ) or homologous recombination (HR) (Chapman et al., 2012). In haploid yeast, NHEJ is prominent only in G1 phase, whereas, in mammals, it dominates throughout the cell cycle (Smeenk and van Attikum, 2013). Repair by HR requires a homologous donor that serves as a template for DNA synthesis, being most commonly provided by the replicated sister chromatid. The choice of repair by HR over NHEJ is dictated in part by 5′ to 3′ end resection at the break, which requires the activity of the S-phase cyclin-dependent kinase (Ira et al., 2004). The resulting single-stranded DNA (ssDNA) overhang is coated by replication protein A (RPA) and later by the Rad51 recombinase. This ssDNA-Rad51 nucleoprotein filament mediates homology search and strand invasion, enabling error-free, recombination-mediated repair. Other less-precise, recombination-based events can also occur, including break-induced replication or template switching, particularly at damaged replication forks (Aguilera and García-Muse, 2013).

Recent work has highlighted the importance of ATP-dependent chromatin remodelers in DSB repair. In yeast, the remodeler complexes RSC and INO80 and the SWR1 complex (SWR-C) are sequentially recruited to breaks, whereas, in mammalian cells, the SWI/SNF homolog as well as INO80 and SRCAP are implicated in repair pathway choice and outcome (reviewed in Peterson and Almouzni, 2013; Price and D'Andrea, 2013; Seeber et al., 2013b; Smeenk and van Attikum, 2013). The budding yeast complexes INO80 and SWR-C accumulate at breaks at much higher levels in S and G2 than G1, coincident with end resection and Rad51 binding (Bennett et al., 2013). Indeed, the recruitment of INO80 facilitates short-range resection at DSBs and Rad51 binding, possibly because of the preferential eviction of H2A.Z-containing nucleosomes (Papamichos-Chronakis et al., 2011; Tsukuda et al., 2005; van Attikum et al., 2004, 2007). More recent work implicates the FUN30 remodeler in long-range end resection (Chen et al., 2012; Costelloe et al., 2012). In contrast, SWR-C exchanges H2A-H2B dimers for Htz1-H2B at promoters, telomeres, centromeres, and, in some cases, DSBs, but its loss does not impair end resection (Kobor et al., 2004; Krogan et al., 2003; Luk et al., 2010; Mizuguchi et al., 2004; Papamichos-Chronakis et al., 2006; van Attikum et al., 2007; Wu et al., 2005). Instead, SWR-C appears to promote the association of yeast Ku to broken ends, facilitating error-free NHEJ (van Attikum et al., 2007). INO80, on the other hand, was shown to facilitate replication fork restart after stalling or collapse of replication forks (Papamichos-Chronakis and Peterson, 2008; Shimada et al., 2008).

Another intriguing effect of chromatin remodeler recruitment to DSBs is the enhanced subdiffusive movement scored for

fluorescently tagged DSBs in yeast (Dion et al., 2012; Miné-Hattab and Rothstein, 2012; Neumann et al., 2012). Not only the site of damage, but other tagged loci throughout the genome showed a general increase in mobility after DSB induction in a manner dependent on checkpoint response and the INO80 remodeler (Neumann et al., 2012; Seeber et al., 2013a). Other studies established that DSBs, which lack a functional donor for HR shift at least transiently to the nuclear periphery, where they appear to bind either the Nup84 nuclear pore subcomplex or an essential inner nuclear membrane Sad1-Unc-84-related (SUN) domain protein Mps3 (Kalocsay et al., 2009; Nagai et al., 2008; Oza et al., 2009; Oza and Peterson, 2010). Fluorescence microscopy confirmed that critically short telomeres and collapsed replication forks associate with nuclear pores (Khadaroo et al., 2009; Nagai et al., 2008), yet it has remained unclear whether Mps3 and pores constitute independent or interdependent sites of DSB interaction. Moreover, it was unresolved what relationship, if any, exists between the enhanced subdiffusive movement that stems from damage and the localization of DSBs to the inner nuclear membrane (INM).

Previous work from our laboratory has shown that Mps3 and nuclear pores distribute independently around the nuclear rim in vegetatively growing cells (Horigome et al., 2011). Unlike Mps3, nuclear pores harbor the SUMO protease Ulp1 and the heterodimeric SUMO-dependent ubiquitin ligase Slx5—Slx8 (Nagai et al., 2008; Zhao et al., 2004; Palancade et al., 2007), which is implicated in alternative recombination-mediated pathways of repair (Khadaroo et al., 2009; Nagai et al., 2008). In contrast, Mps3 was shown to sequester DSBs from promiscuous interactions with chromatin and suppress telomere-telomere recombination in mutant strains (Oza et al., 2009; Schober et al., 2009). These results provide indirect arguments that these DSB binding sites have different functions, yet it is unclear what differentiates one binding site from the other.

Here, we combine chromatin immunoprecipitation (ChIP) and fluorescence imaging approaches in appropriate mutant backgrounds in order to distinguish and characterize the two DSB binding sites at the nuclear envelope. We find cell-cycle-dependent binding site selection with differential dependence on the INO80 chromatin remodeler. On the other hand, the related SWR-C and its deposition of Htz1 were required for relocation to both sites. By studying factors that affect DSB mobility, we also distinguish perinuclear binding site choice from DNA-damage-response-enhanced mobility. Finally, we confirm that mutants that ablate one or the other binding site have distinct outcomes on repair, arguing that the spatial segregation of damage participates selectively in pathways of repair.

RESULTS

SWR-C-Dependent H2A.Z Incorporation Is Required to Shift a DSB to the Nuclear Periphery

To study the relocation of damaged DNA to the nuclear periphery, we used a strain in which a unique DSB can be induced at the mating type locus (*MAT*) by galactose-controlled expression of the homothallic (HO) endonuclease. The donor sequences at *HML* and *HMR* are deleted in order to prevent intrachromosomal repair by gene conversion (Figure 1A). To determine the subnuclear localization of the DSB, we inserted an array of *lacO* sites at 4.4 kb from *MAT* and expressed a GFP-LacI fusion and either a GFP- or cyan fluorescent protein (CFP)-tagged pore protein (Figures 1A and 1B). In wild-type (WT) cells exposed to galactose for 2 hr, the induced DSB shifts efficiently to the nuclear periphery, and 59% of the cleavage sites mapped to the outermost rim (zone 1; 52% in WT CFP-Nup49-expressing strains; $p < 1.0 \times 10^{-30}$ or $p = 1.2 \times 10^{-11}$ versus random; Figures 1C and 1E; Table S3 available online). On the other hand, the uncleaved *MAT* locus has a random subnuclear localization (Figure 1C) (Nagai et al., 2008).

Histone variant Htz1 is deposited at DSBs, and its loss was shown to abolish the association of the break with Mps3 in S or G2-phase cells (Kalocsay et al., 2009). Although Htz1 physically interacts with Mps3 in vitro, recent work showed that Htz1 also serves as an essential chaperone for the insertion of Mps3 into the INM (Gardner et al., 2011). Thus, the negative effect of *htz1* deletion on DSB localization could stem from a failure to integrate Mps3 into the INM and not an absence of Htz1 at the break. To resolve this issue, we made use of a mutant called *htz1ΔM6* (Wu et al., 2005), which ensures proper INM localization of Mps3 but fails to bind SWR-C. Therefore, the mutant histone htz1ΔM6 is not incorporated into chromatin by SWR-C (Gardner et al., 2011; Wu et al., 2005). We confirmed that the cleaved *MAT* locus failed to shift to the nuclear periphery in the *htz1Δ* strain and that relocation could be faithfully restored by expression of WT Htz1 (Figure 1D). However, the mutant histone htz1ΔM6 failed to support break relocation to the nuclear rim (Figure 1D). This, along with the fact that either loss of Swr1 or the SWR-C component Arp6 completely eliminated DSB relocation to the nuclear periphery (Figure 1E), argued strongly that the deposition of Htz1 at damage by SWR-C is indeed crucial for DSB relocation. Consistently, complementation of the *swr1Δ* background with a WT *SWR1* gene (+*SWR1*; Figure 1F), but not the catalytic site mutation (+ s*wr1K727G*; Figure 1F), restored relocation of the DSB to the nuclear periphery, demonstrating dependence on both SWR-C and Htz1 deposition.

Although SWR-C is implicated in Htz1 incorporation, INO80 has been proposed to remove this histone variant at both damage and other sites (Kobor et al., 2004; Krogan et al., 2003; Luk et al., 2010; Mizuguchi et al., 2004; Papamichos-Chronakis et al., 2006; van Attikum et al., 2007; Wu et al., 2005). To see whether the importance of Htz1 deposition by SWR-C is to recruit INO80 to breaks, we examined whether ablation of the INO80 chromatin remodelling complex would affect DSB relocation. Because *ino80Δ* itself is lethal in our yeast background, we instead tested the effects of *arp5Δ* or *arp8Δ* mutants, which compromise INO80-remodelling activity and reduce INO80 recruitment to breaks (Shen et al., 2000; van Attikum et al., 2004). Surprisingly, there was no effect of *arp5* or *arp8* deletion on DSB relocation (Figure 1E).

INO80 has been implicated in the removal of nucleosomes to favor resection at DSBs, whereas *swr1* mutants showed no defect in resection (van Attikum et al., 2007; Chen et al., 2012). Although resection is not sufficient for relocation, it leads to the binding of Rad51, which, along with Rad52, was shown to be necessary for the detection of damaged DNA at Mps3 by ChIP

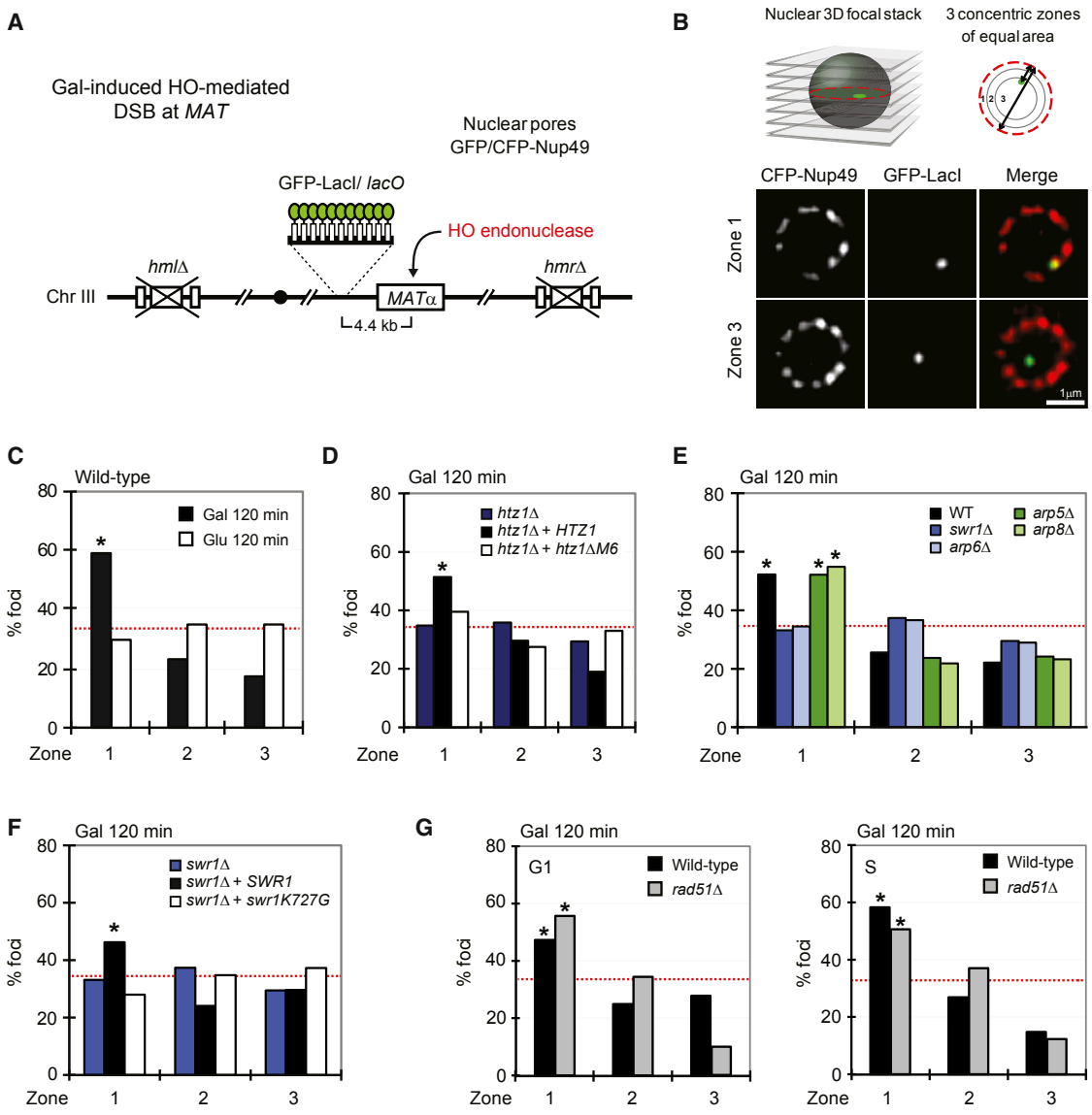

Figure 1. SWR1-Dependent H2A.Z Incorporation Is Required to Shift DSBs to the Nuclear Periphery

(A) Shown is Chr III in strains GA-1496 and GA-6844 bearing deleted homologous donor loci (*hml*Δ/*hmr*Δ) and a *lacO* array 4.4 kb from the HO cut site at *MAT*, which allows visualization by GFP-LacI. Pores are visualized by GFP-Nup49 (GA-1496) or CFP-Nup49 (GA-6844).

(B) Locus position is scored relative to the nuclear diameter in its plane of focus, as described in the Supplemental Information. Distance over diameter ratios are binned into three equal zones. 33% distribution = random.

(C) *MAT* position in GA-1496 (WT) after 120 min on galactose (Gal) or glucose (Glu). * = significantly nonrandom distribution on the basis of cell number and confidence values from a proportional test between random and experimental distribution (see Table S3).

(D) In strain GA-7095 expressing *HTZ1* or *htz1*Δ*M6* from the *HTZ1* promoter at *URA3*, *MAT* position was scored at 120 min on galactose as in C. Strains: *htz1*Δ (GA-7095), *htz1*Δ + *HTZ1* (GA-8110), and *htz1*Δ + *htz1*Δ*M6* (GA-8111).

(E) *MAT* position relative to CFP-Nup49 in WT (GA-6844), *swr1*Δ (GA-7003), *arp6*Δ (GA-7094), *arp5*Δ (GA-8069), and *arp8*Δ (GA-7103) as in (C) and (D).

(F) In *swr1*Δ (GA-7003) strain or same expressing *SWR1* or *swr1K727G* from a *TEF* promoter, *MAT* position was scored as in (C) and (D). *swr1*Δ (GA-7003), *swr1*Δ + *SWR1* (GA-8667), and *swr1*Δ + *swr1K727G* (GA-8668).

(G) *MAT* position scored in WT (GA-6844) and *rad51*Δ (GA-7099) cells as in (C) and (D) but binned into G1 (unbudded) and S (budded) cells.

See also Figure S1.

(Kalocsay et al., 2009; Oza et al., 2009). Using our quantitative positioning assay, we tested whether Rad51 or Rad52 was necessary for the perinuclear relocation of the DSB. Surprisingly, and in contrast to Mps3-ChIP results (Kalocsay et al., 2009), we scored a significant enrichment of the DSB at the nuclear periphery in both *rad51*Δ and *rad52*Δ mutants (Figures 1G and S1). Altogether, these results led us to propose that in addition to Mps3, a Rad51-independent DSB binding site, should exist at

the nuclear periphery. The obvious candidate for this would be the Nup84 subcomplex of the nuclear pore, which was shown by ChIP and fluorescence microscopy to interact with irreparable DSBs in an asynchronous population of cells (Nagai et al., 2008).

Although Kalocsay et al. (2009) claimed that they could not distinguish between pore and Mps3 binding by ChIP, the two INM complexes are indeed distinct by high-resolution fluorescence microscopy (Horigome et al., 2011). In WT cells, endogenously tagged Mps3 (EGFP-Mps3; Figure 2A) shows a bright focus at the spindle pole body (SPB; Figure 2A, arrow) and a weak perinuclear ring. To see whether the weak Mps3 rim staining was pore dependent, we induced the clustering of nuclear pores by deleting a portion of the N-terminal domain of Nup133 (Δ amino acids [aa] 44–236) (Doye et al., 1994). In this mutant, pores cluster without loss of function. However, the EGFP-tagged Mps3 retained its rim staining (Figure 2A, red = pore, green = Mps3), even though the bright SPB was often adjacent to a pore cluster. The independence of the non-SPB Mps3 signals from pores reinforced the hypothesis that the Rad51-independent perinuclear localization of DSBs might reflect their association with pores.

To correlate nuclear pore and/or Mps3 binding with the effects of the mutations described in Figure 1, we performed ChIP assays with Mab414 (antinuclear pore) and anti-HA (recognizing 3HA-Mps3) in WT and mutant yeast strains (Figure 2B). Consistent with previous work, an induced DSB could be recovered in immunoprecipitates for either nuclear pore or Mps3 in WT cells (Figure 2B). The level of association increased rapidly for 120 min after cut induction before reaching a plateau. In *swr1*Δ strains, break association with either pores or Mps3 was reduced to a background level, which existed prior to HO induction. Thus, ChIP confirms that the SWR-C is required for DSB relocation.

In contrast, in the INO80-deficient *arp8*Δ strain, DSB association with the nuclear pore occurred at WT levels, whereas break binding to Mps3 was lost (Figure 2B). Thus, the binding of DSBs to Mps3, but not pores, requires INO80 activity. The fact the breaks bind pores in the absence of INO80 is consistent with the INM-localization of the DSB in *arp5*Δ and *arp8*Δ strains, as presented in Figure 1. Given that break association with either the pore or Mps3 required SWR-C, the action of INO80 appears to distinguish damage that is destined for Mps3 from damage that is targeted to pores. This could reflect either the direct binding of INO80 or an alteration of the DSB that is INO80-dependent and renders the DSB able to bind Mps3.

Microscopic Confirmation that INO80 Contributes Only to DSB-Mps3 Association

We sought to confirm this finding with an assay that does not depend on protein-DNA crosslinking, given that formaldehyde crosslinking efficiency varies significantly from protein to protein. To achieve this, we scored for colocalization of a GFP-LacI-tagged DSB and CFP-tagged nuclear pores with high-resolution spinning disk confocal microscopy. To enhance the accuracy of scoring colocalization by microscopy, we used a *nup133*Δ*N* background, in which pores form a large, single cluster (Doye et al., 1994). The deletion of the Nup133 N terminus does not affect macromolecular import or export and does not confer sensitivity to DNA-damaging agents, unlike complete loss of Nup133 or Nup84 subcomplex components (Doye et al., 1994; Loeillet et al., 2005). We scored three degrees of colocalization with the pore cluster: fully overlapping, partially overlapping, and juxtaposition (“touching”; Figure 2C). All three degrees of colocalization are consistent with molecular interaction of the break with the pore cluster, given the relative signal sizes of the *lacO* array and the clustered pore (Schober et al., 2009).

The background level of colocalization was determined with a strain that lacks the gene for the HO endonuclease (*ho*Δ). In this strain, we found *MAT* juxtaposed to a pore cluster in 20% of the cells, and this value did not change over time. This background is higher than the computed likelihood of a *lacO* focus coinciding with the pore cluster (9%) (see Schober et al., 2009). Nonetheless, we use this empirically determined value as the background above which colocalization of the DSB and pore is considered significant (Figures 2C–2E, *ho*Δ).

In a WT yeast strains, DSB colocalization with pores showed a rapid increase upon induction of cleavage, which was then reduced to a plateau of 30% (Figure 2C). This could indicate that DSB binding at pores is transient for a subpopulation of breaks or else that extensive resection at the break eliminates the *lacO* signal at later time points (Figure S2). Nonetheless, there was significant colocalization of DSBs with the pore cluster in both G1- and S-phase cells (Figure 2D). Importantly, DSB-pore interaction was diminished in *swr1*Δ, but not *arp8*Δ, strains, providing independent confirmation that pore association of a DSB requires SWR-C but not a functional INO80 complex. The slight delay in DSB accumulation at pores in the *arp8*Δ strain correlates with both reduced chromatin mobility and reduced resection rate at the break in that mutant (Neumann et al., 2012; van Attikum et al., 2007). In conclusion, quantitative microscopy confirms a differential requirement for SWR-C and INO80 in the association of DSBs with pores.

Another variable in break relocalization is the stage of the cell cycle at which position is measured. In previous ChIP studies, the Mps3-DSB interaction was detected in asynchronous cultures, yet it was lost when cells were arrested in G1 (Kalocsay et al., 2009). Cell-cycle effects were not examined in the context of DSB association with pores. Taking advantage of the ease with which one can determine cell-cycle stage by yeast cell morphology, we binned the cells scored by microscopy into unbudded (G1 phase) and budded cells, counting only those in which the nuclei were still round (early to mid S phase) (Figure 2D). We conclude from this that DSB-pore interaction occurs in both G1- and S-phase cells, reaching 36% and 43% colocalization with pores, respectively. In both sets of cells, pore association depends on SWR-C (Figure 2D) and cleavage (Figure 2E, *ho*Δ background, ~20%). However, in S phase, DSB association with the pore was independent of INO80 function, and even increased in the absence of Arp8 (Figure 2D). Moreover, whereas Mps3 binding was reported to be sensitive to loss of Rad51 (Kalocsay et al., 2009; Oza et al., 2009), we found that DSB-pore association was intact in the *rad51*Δ mutant (Figure 2D). Thus pore-DSB interaction occurs in G1- and S-phase cells and is dependent on SWR-C but independent of Rad51 and INO80. On the other hand, DSB recruitment to Mps3 requires Rad51 and INO80 and is restricted to S phase.

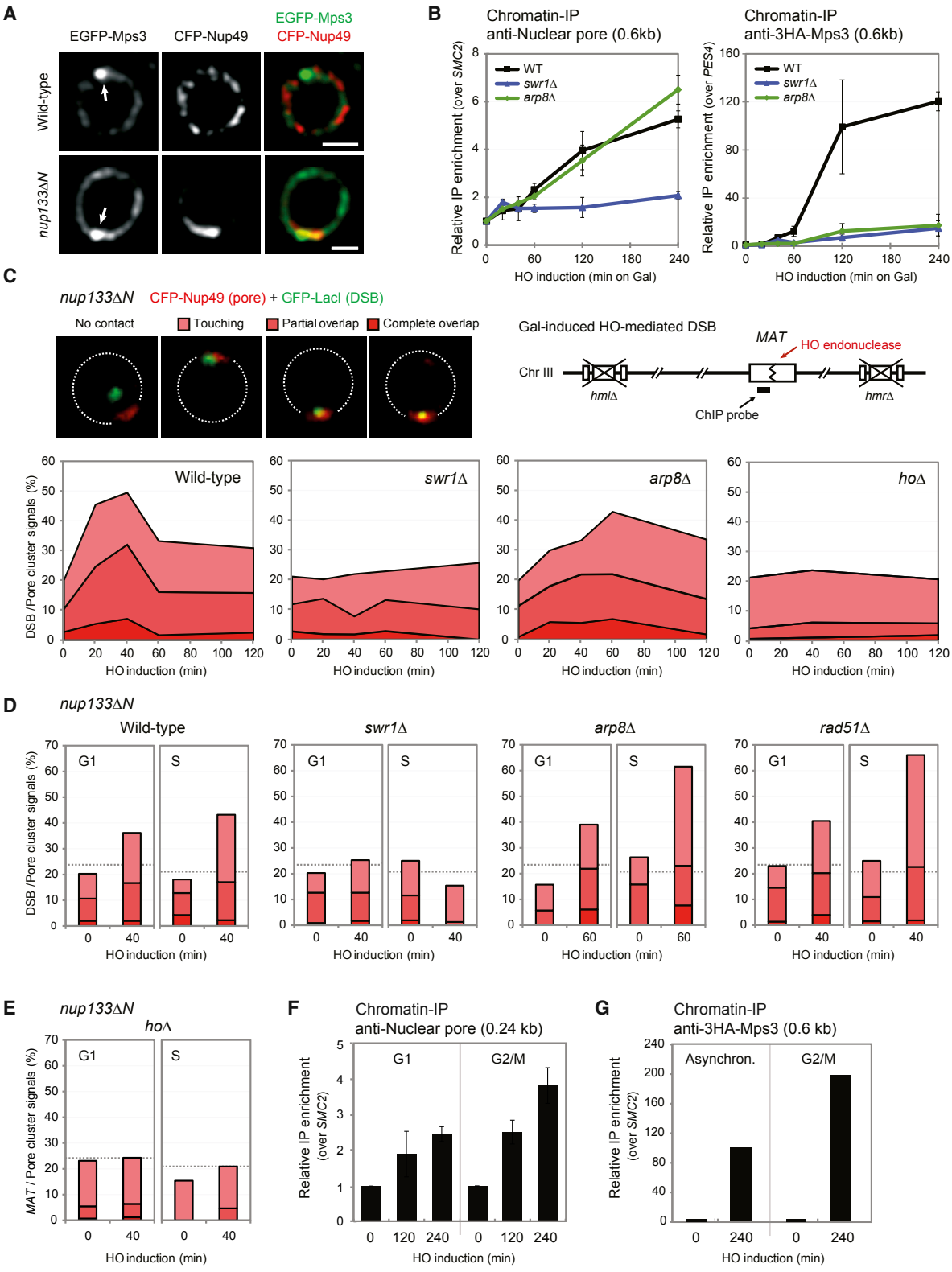

Figure 2. SWR-C Is Required for DSB Binding at Both Nuclear Pores and Mps3, and INO80 Is Only Required for Mps3 Interaction

(A) EGFP-Mps3 and CFP-Nup49 localization in WT (GA-6647) and in pore-clustering cells (*nup133ΔN*, GA-6650). Images are reproduced from (Horigome et al., 2011) with permission. Arrow = spindle pole body; white bars = 1 μm.

(legend continued on next page)

To make sure that these cell-cycle conclusions were not artifacts of the *nup133ΔN* strain, we confirmed them with ChIP assays for nuclear pore proteins (Mab414, see the Experimental Procedures) and HA-tagged Mps3 in synchronized *NUP133*$^{+}$ cells. Cells arrested in G1 showed a cleavage-dependent increase in association with nuclear pores but not Mps3 (Figures 2F and 2G) (Kalocsay et al., 2009; Oza et al., 2009). Both types of association increased in G2- and M-phase cells (Figures 2F and 2G). This contrasts with the fluorescence colocalization analysis, where we scored a drop in DSB-pore interaction in both WT and *arp8Δ* cells at 120 min after cut induction (Figure S2A). Given that this correlates with a reduced number of bright LacI/*lacO* foci (<1 per cell), we suggest that the drop in colocalization stems from resection through the *lacO* repeat sequence at 120 min postcleavage (Figures 2A and 2B). Intriguingly, in both *rad51Δ* and *arp8Δ* cells, DSBs bind more efficiently to pores in S-phase than WT cells, even though the Mps3 interaction drops in these mutants. This is consistent with the two binding sites being competitive, rather than sequential binding sites.

Htz1 Is Able to Mediate Direct Interaction with Mps3 but Not Nuclear Pores

The loss of perinuclear interactions in remodeler deletion strains does not necessarily mean that the remodeler itself mediates interaction with pores or Mps3. Rather, the effects could be achieved indirectly by the action of the complex on the substrate; i.e., modification of chromatin or processing of the DSB. However, in the case of Htz1, it was proposed that this histone variant interacts directly either with nuclear pores (Dilworth et al., 2005; Light et al., 2010) or Mps3 (Gardner et al., 2011). To test whether Htz1 incorporation is sufficient to shift chromatin to either nuclear pores, Mps3, or both, we made use of a gain-of-function assay in which LexA fusion proteins are targeted to four double LexA operators inserted near a fluorescently labeled locus (ARS607). Then, subnuclear position of ARS607 was monitored in the absence of DNA damage. This locus has a random subnuclear localization even when LacI/*lacO* is near it, and, consistent with previous work, the binding of LexA does not alter its random distribution (Taddei et al., 2004) (open bars, Figures 3A–3C). On the other hand, the binding of LexA fused to a protein that has affinity for an INM protein shifts ARS607 in a statistically significant manner to zone 1, which is the case for LexA-Htz1 in both WT and *swr1Δ* cells (Figures 3B and 3C). Moreover, LexA-htz1ΔM6, which cannot bind SWR-C, worked as efficiently as LexA-Htz1 itself in translocation (Figure 3B). Not surprisingly, these interactions were cell-cycle independent.

Next, we asked whether the Htz1-mediated interaction with the nuclear periphery reflects binding to nuclear pore complexes, as had been previously shown for LexA-Arp6 (Yoshida et al., 2010). To score this, we targeted LexA-htz1ΔM6 to the LexA/*lacO*-tagged *LYS2* in a *nup133ΔN* background expressing CFP-Nup49 and scored colocalization of *LYS2* with the pore cluster. LexA-htz1ΔM6 was unable to enhance interaction with the nuclear pores above background levels (20%), whereas the targeting of LexA-Swr1 could (Figure 3D). Finally, to see whether Htz1 functions by binding Mps3, we overexpressed the nucleoplasmic N-terminal domain of Mps3, which distributes throughout the nucleoplasm (Schober et al., 2009), along with LexA- htz1ΔM6. In this case, LexA-htz1ΔM6 no longer shifted ARS607 to zone 1 in either WT or *swr1Δ* cells (Figure 3E), suggesting that the soluble Mps3N competes for Htz1-Mps3 interaction at the INM. Unfortunately, we were unable to test an *mps3ΔN* mutant in this assay, given that the cells show severely impaired growth (data not shown). In conclusion, the targeting of a LexA-Htz1 fusion is sufficient to shift chromatin to the INM in the absence of damage, probably because of its affinity for Mps3N. Previous work showed that LexA-Arp6 can shift an internal LexA-tagged locus to the nuclear pore cluster (Yoshida et al., 2010) as we show here for LexA-Swr1 (Figure 3D). The significance of this Swr1 interaction for DSB relocalization is unclear, given that we showed above that point mutants that eliminate the ATPase activity of SWR-C blocked DSB relocation (Figure 1F). In summary, we suggest that SWR-C functions in DSB relocation in multiple interdependent ways: by depositing Htz1, by serving as a bridge for pore interaction, and possibly by enhancing the subdiffusive mobility of chromatin in response to breaks (Dion et al., 2012; Miné-Hattab and Rothstein, 2012).

Testing the Role of Remodeler-Enhanced DSB Mobility in DSB Relocalization

Previous work demonstrated a role for INO80 remodeling activity in chromatin movement both at a DSB and when targeted to undamaged sites (Neumann et al., 2012), whereas the role of SWR-C or Htz1 deposition had not been tested. To examine this, we scored the mobility of a *lacO*-tagged induced DSB at the *ZWF1* locus in the middle of the long left arm of chromosome XIV in *swr1*- and *htz1*-deficient strains (Figure 4A). The deletion of *swr1* did not affect in the mobility of the locus in the absence of damage (Figure 4B); however, after I-SceI-induced cleavage, the dramatic increase in DSB movement that occurs in WT cells was compromised in *swr1*- and *htz1*-deficient strains (Figure 4C). The effect was similar in the absence of other SWR-C subunits,

(B) Top: ChIP against nuclear pores (Mab414) and 3HA-Mps3 (anti-HA) at the indicated times on galactose. Enrichment of *MAT* (0.6 kb from the cut site) over uncut *SMC2* or *PES4* was quantified with quantitative PCR in WT (GA-7002), *swr1Δ* (GA-7004), and *arp8Δ* (GA-7161) cells. Bottom: ChrIII in strains used.
(C) Scoring of *MAT* colocalization with the pore cluster in *nup133ΔN* (GA-7314) after cut induction as shown in WT (GA-7314), *swr1Δ* (GA-8142), *arp8Δ* (GA-8143), and *hoΔ* (GA-8669) cells. Scored at indicated times on galactose. Pink/red shaded region = colocalization; *hoΔ* values = background.
(D and E) Experiments performed as in (C) with data binned into G1- or S-phase cells. Strains are the same as in (C) plus *rad51Δ* (GA-8072) with *nup133ΔN*. Dotted line = background (see *hoΔ*).
(F) ChIP analysis performed as in (B) on galactose with Mab414 in WT (GA-8627) cells. Cells were synchronized in G1 phase by α factor and in G2 and M phase by nocodazole. PCR primers for *MAT*a are 0.24 kb from cut site. Enrichment over an uncut *SMC2* locus was calculated and normalized to 0 min Gal and cut efficiency.
(G) ChIP analysis at 0 or 240 min on galactose for 3HA-Mps3 and at *MAT*α in WT (GA-7002) cells as in (B). Cells are asynchronous or synchronized in G2 and M phase by nocodazole. Enrichment was calculated as in (F), and data from multiple experiments are represented as mean ± SEM.
See also Figure S2.

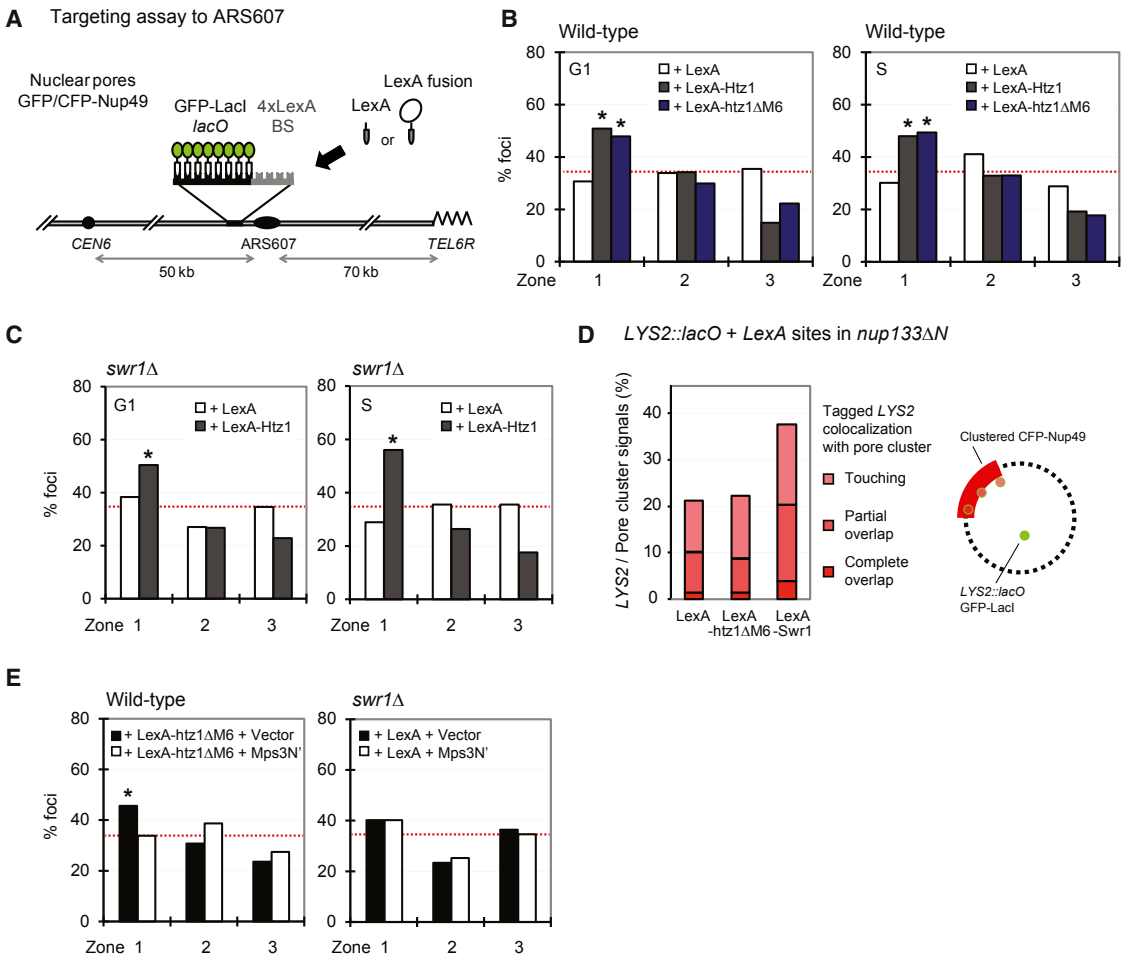

Figure 3. Htz1 Is Sufficient to Shift an Internal Locus to the Nuclear Periphery

(A) The position of *lacO*/LexA-tagged ARS607 was visualized by GFP-LacI and scored as in Figure 1B. Cells are binned into G1 or S phase as in Figure 1G. Strains carry either GFP-Nup49 (GA-1461) or CFP-Nup49 (GA-1993). LexA fusion proteins are expressed from plasmids.

(B) WT strain (GA-1993) expresses indicated LexA fusion constructs. ARS607 position was scored as in (A).

(C) Experiments were performed as in (B) with strain bearing *swr1*Δ (GA-7898).

(D) Pore cluster colocalization for LexA-tagged *LYS2* in a strain bearing *nup133ΔN* (GA-4584) transformed with LexA fusions. Colocalization (pink to red) is presented as in Figure 2C.

(E) In a WT strain (GA-1993) expressing LexA-htz1ΔM6 and Mps3N′, ARS607 position was scored as in (B). Right, same experiments performed with *swr1*Δ (GA-7898) bearing LexA and either an empty vector or the Mps3N′ construct.

Swc2 and Swc5 (Figure S3), which are necessary for remodeler function (Wu et al., 2005). The reduction in mobility was as strong as, if not stronger than, the reduced mobility of the same DSB in *arp8*Δ or *rad51*Δ mutants (Figure 4D) (results from Dion et al., 2012; Neumann et al., 2012). However, in *arp8*Δ or *rad51*Δ strains, we still score the shift of DSBs to the INM (Figures 1 and 2), ruling out an absolute requirement of enhanced mobility for relocation to pores.

Having demonstrated that the LexA-mediated targeting of Swr1, Arp6, and Htz1 can mediate relocation to the nuclear periphery, we tested whether they also affect the mobility of the undamaged locus to which they are bound. We find that the expression of LexA-Arp6, LexA-Htz1, or LexA-htz1ΔM6 confers no significant increase in ARS607 mobility (Figures 4E and 4F), yet they can still shift the locus to the INM (Figure 3). Indeed, the targeting of LexA-Arp6, which can bring an internal locus to pores (Yoshida et al., 2010), reduces ARS607 mobility (Figure 4E). Given that LexA-Arp5, LexA-Arp8, or LexA-Ino80 bound to various undamaged sites enhance locus mobility (Neumann et al., 2012) and do not lead to perinuclear enrichment (Figure S4), we conclude that enhanced random movement is neither sufficient nor necessary for shifting a DSB to the INM.

Crosstalk between Anchorage at Pores and Mps3 Reveals Additive Phenotypes

We have distinguished the two INM binding sites for DSBs with respect to INO80 and cell-cycle dependence, yet it remained possible that the two sites influence each other in some way. For example, pore binding might precede binding to Mps3 or

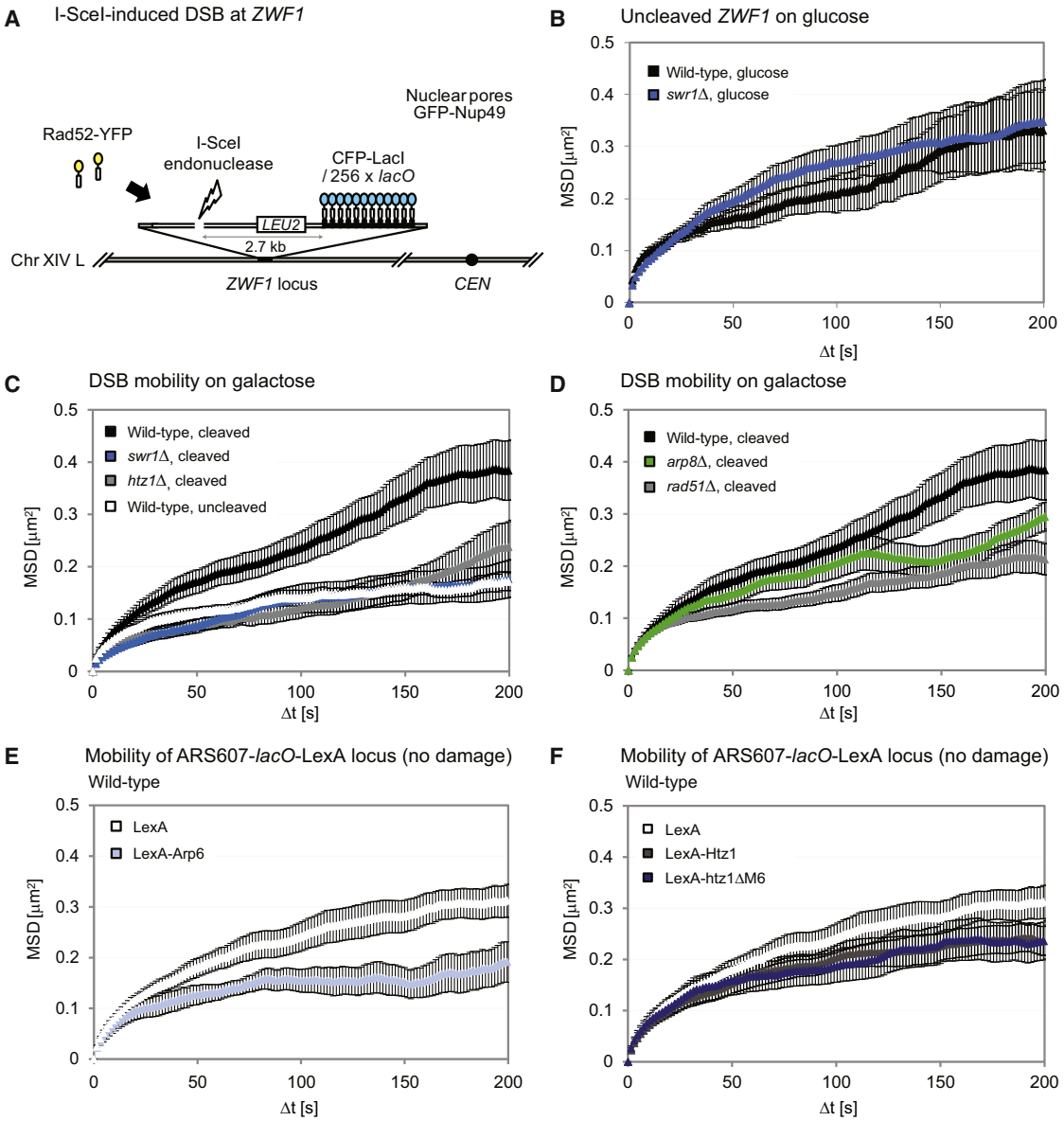

Figure 4. Enhanced DSB Mobility Depends on SWR-C and H2A.Z but Is Not Required for Relocalization

(A) Schematic representations of the I-SceI cut site and a *lacO* array inserted at *ZWF1* on chromosome 14L (GA-6208). Strains express CFP-LacI and galactose-induced I-SceI from a 2 μm plasmid.

(B) MSD plots (see the Experimental Procedures) of the *ZWF1* locus in WT and *swr1*Δ cells during S phase in glucose medium show no mobility change for undamaged chromatin in *swr1*Δ.

(C) MSD plots of I-SceI-induced Rad52-YFP foci in WT (GA-6208), *swr1*Δ (GA-6335), *htz1*Δ (GA-6637) strains, and CFP-LacI at uncut site (GA-6215) during S phase. Only the cut WT sample increases mobility.

(D) MSD plots of I-SceI-induced Rad52-YFP foci in WT (GA-6208), *arp8*Δ (GA-6317), and *rad51*Δ (GA-6225) strains during S phase reproduced with permission (Dion et al., 2012; Neumann et al., 2012).

(E and F) MSD plots of the undamaged *lacO*/LexA-tagged ARS607 tracked after binding LexA or the indicated LexA fusion during G1 phase. The reduction in mobility due to Arp6 binding is significant. MSD data are represented as mean ± SEM.

See also Figures S3 and S4.

vice versa. This was tested directly by monitoring DSB relocation in mutants lacking one or the other site.

Consistent with earlier findings (Oza et al., 2009), we show through both microscopic analysis and ChIP that DSBs fail to relocate to the nuclear periphery in the *mps3Δ65-145* strain (Figures 5A–5C). Interestingly, the relocation defect in the *mps3Δ65-145* strain was observed in both G1- and S-phase cells, even though DSB binding to Mps3 is only detected in G1 (Kalocsay et al., 2009). Using the colocalization assay, we confirmed that a GFP-tagged DSB failed to bind the CFP-labeled

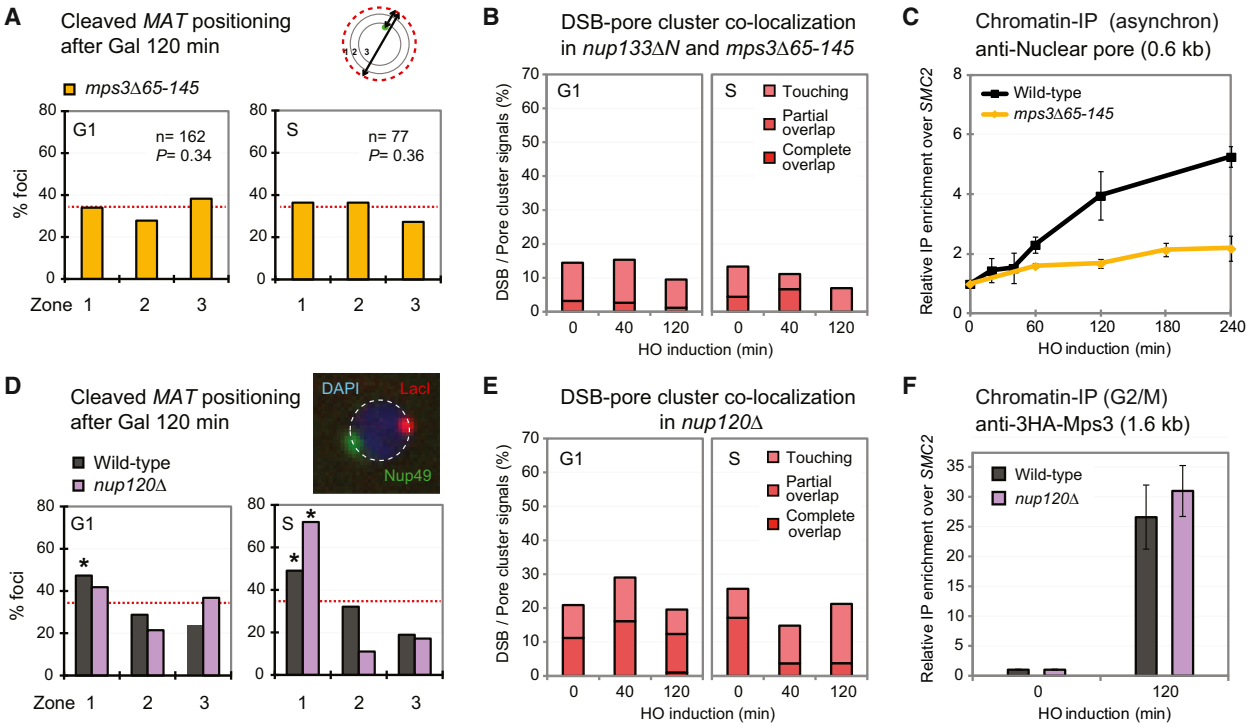

Figure 5. Nonreciprocal Effects of the Loss of Mps3N or of Nup120 on DSB Positioning

(A) Position of cleaved *MAT* loci in *mps3Δ65-145* (GA-7096) scored at 120 min after HO induction as in Figure 1G.

(B) Colocalization of the nuclear pore cluster and the *MAT* scored for G1 or S phase in *mps3Δ65-145* cells with *nup133ΔN* (GA-7897). Quantified as in Figure 2D.

(C) ChIP for nuclear pores (Mab414) after the indicated time on galactose in WT (GA-7002) and *mps3Δ65-145* cells (GA-7096). Quantitation and enrichment over *SMC2* was normalized as in Figure 2B. Data from multiple experiments are represented as mean ± SEM.

(D) GFP-tagged *MAT* position was determined in WT (GA-6844) and *nup120Δ* (GA-8141) relative to the nuclear periphery determined from DAPI staining as in Figure 1G. An S-phase *nup120Δ* cell nucleus is shown.

(E) *MAT* colocalization with nuclear pores scored in G1- or S-phase *nup120Δ* cells (GA-8141) as in (B).

(F) ChIP for 3HA-Mps3 monitors *MAT* locus after 120 min on galactose in WT (GA-8306) and *nup120Δ* (GA-8308) cells synchronized in G2 and M phase by nocodazole. Enrichment by quantitative PCR as in Figure 2B but with a probe that recognizes both mating-type alleles (1.6 kb from cut site). ChIP data are mean ± SEM.

See also Figure S5.

pore cluster in *nup133ΔN* in the absence of the Mps3 N terminus in both G1- and S-phase cells (Figure 5B). This did not reflect obvious pore misdistribution (Figure S5). The effects were confirmed by nuclear pore ChIP on the cleaved *MAT* locus: loss of Mps3N reduces break-induced association with pores from 5- to 2-fold (Figure 5C).

To test whether this crosstalk was reciprocal or not, we scored for the effect of deleting a component of the Nup84 subcomplex on DSB relocation to Mps3. The short arms of the Nup84 Y-shaped complex mediate key contacts with components of the nuclear pore complex, and these are lost upon deletion of any Nup84 subcomplex component (Fernandez-Martinez et al., 2012). Therefore, we used a strain lacking Nup120, which disrupts DSB interaction with the pore (Nagai et al., 2008). Importantly, in this mutant, we found that DSB relocation to the nuclear periphery is lost in G1- phase, but not S-phase, cells (Figure 5D). We could prove that this mutant disrupts interaction with the nuclear pore by scoring colocalization of the tagged DSB with the CFP-labeled pore cluster in *nup120Δ* cells. As expected, cleavage-induced association with the nuclear pore cluster was lost upon ablation of Nup120 in both G1- and S-phase cells (Figure 5E). On the other hand, Mps3 ChIP showed WT levels of DSB association with 3HA-Mps3 in the absence of Nup120 (Figure 5F). Thus, Mps3 influences DSB binding to pores but not vice versa.

Repair Defects in *mps3* or Pore Mutants Are Additive

To test whether interactions at the two binding sites are functionally epistatic or additive for repair, we constructed double mutants that compromise the Nup84 subcomplex (*nup120Δ*) and the Mps3 nuclear anchorage domain (*mps3Δ65-145*). Single and double mutants were challenged with DNA damage. In a simple drop assay that monitors sensitivity to 0.03% methyl methanesulfonate (MMS), we found that the effects of *nup120Δ* and *mps3Δ65-145* on cell viability after plating on MMS were indeed additive (Figure 6A). This suggests that the two anchorage sites mediate different functions under conditions of S phase damage.

To extend this to a more precise pathway of repair, we scored for DSB repair by unequal sister chromatid recombination

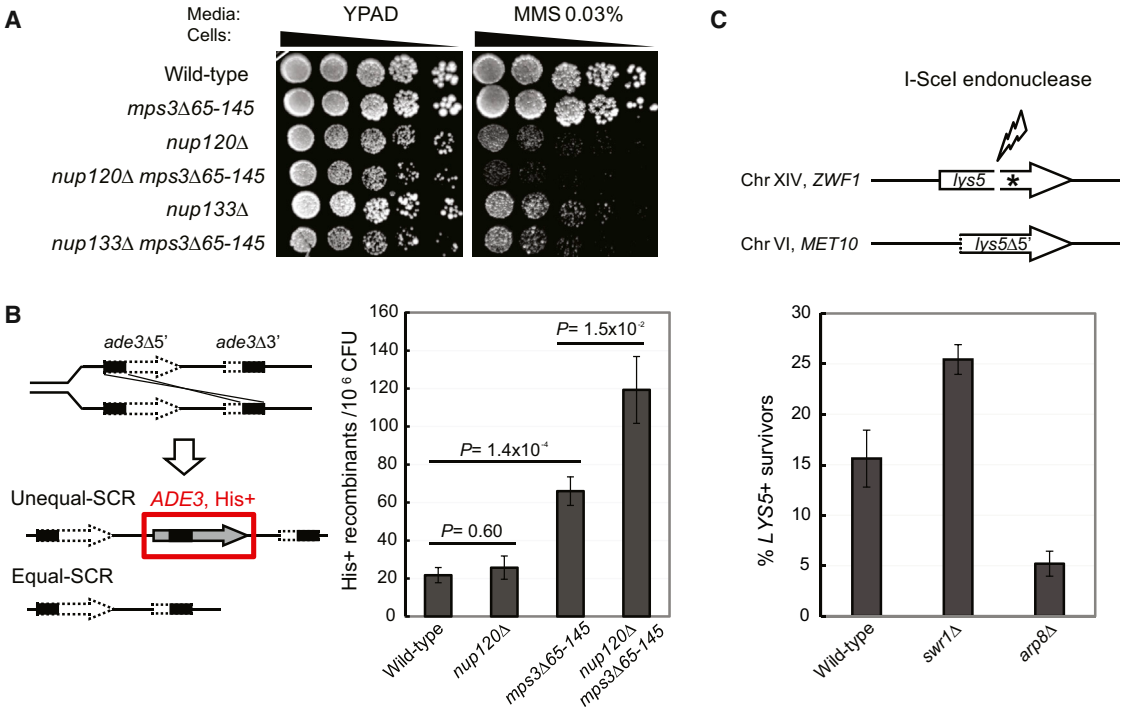

Figure 6. Additive Effects of *nup120* and *mps3* on Unequal Sister Chromatid Exchange

(A) Serial dilutions of isogenic strains bearing indicated mutations (*nup120*Δ or *nup133*Δ and *mps3Δ65-145*) were spotted onto the YPAD ± 0.03% MMS. Plates shown are after 3 days of growth.

(B) The uSCR frequencies of WT (SCRMTL2), *nup120*Δ (YH1301), *mps3Δ65-145* (YH1302), and *nup120*Δ *mps3Δ65-145* (YH1303) cells were determined by plating on YPAD or SC-His medium. Recombination frequency = number of His^+ recombinants per 10^6 colony forming units (CFUs) from eight experiments. Error bars indicate SD.

(C) An I-SceI cut site was placed within the *lys5* gene bearing a frameshift mutation on Chr XIV in a strain with a galactose-inducible I-SceI. An induced DSB repaired by gene conversion with the truncated *lys5* template at *MET10* (Chr VI) allows survival on galactose-Lys plates. Survivors over total plated cells yields the rate of gene conversion. Tested were eight independent colonies of *swr1*Δ (GA-6386), six colonies of *arp8*Δ (GA-6382), and 14 colonies of WT (GA-6217). An *rsc2*Δ strain yielded same as *arp8*Δ (data not shown). Significance was determined by a Student's t test (p = 0.0209; WT versus *swr1*Δ, p = 0.0306; WT versus *arp8*Δ). Error bars indicate SD.

(uSCR) (González-Barrera et al., 2003; Kadyk and Hartwell, 1992, 1993). It has been proposed that uSCR occurs when the replication fork bypasses lesions that normally obstruct its passage. The frequency of uSCR in the absence of Nup120 did not increase significantly over WT frequencies (Figure 6B). However, in the *mps3Δ65-145* mutant, we scored a strong increase in uSCR recombination (Figure 6B). Again, the double mutant showed additive effects, arguing that unequal sister chromatid exchange is indeed repressed by binding to Mps3 (Figure 6B), whereas an alternative pathway of repair appears to be lost by *nup120* deletion. If pore and Mps3 anchorage worked on the same pathway to repress recombination, then the two mutations would have shown epistatic effects on uSCR efficiency.

Finally, we scored for rates of homologous recombination with an ectopic donor at an induced DSB (Figure 6C). We found that loss of SWR-C increases HR with an exact ectopic donor, again confirming that sequestration of a DSB at the INM probably disfavors either homology search or the recombination event (Dion et al., 2012; Oza et al., 2009). As expected, the loss of Arp8 had the opposite effect (Figure 6C), confirming earlier results that scored reduced rates of resection and chromatin mobility in this mutant (van Attikum et al., 2007; Neumann et al., 2012).

DISCUSSION

Many nuclear events have been shown to be localized to nuclear subcompartments, although it has remained unclear what establishes the localization of damage and whether different positions impact repair pathways differentially. Here, we exploited both quantitative microscopy and ChIP studies in order to examine the relocation of DSBs to the nuclear envelope in budding yeast. Although each assay has inherent weaknesses, the combination allows us to show conclusively that the two proposed binding sites for DNA damage, the SUN domain protein Mps3, and the Nup84 subcomplex of the nuclear pore, are distinct DSB binding sites. We resolve apparent contradictions in the literature by showing that DSBs bind pores in both G1 and S-phase cells, whereas they associate with Mps3 only in S and G2. A differential requirement for INO80 and SWR-C remodelers for translocation to Mps3 and pores reinforces the argument that the binding sites are distinct. Furthermore, disruption of the two anchors has differential effects on DSB repair: anchor site loss has additive, and not epistatic, impact on the survival of alkylating damage and for uSCR (Figure 6). Finally, we identified a nonreciprocal crosstalk between the Mps3 N terminus and

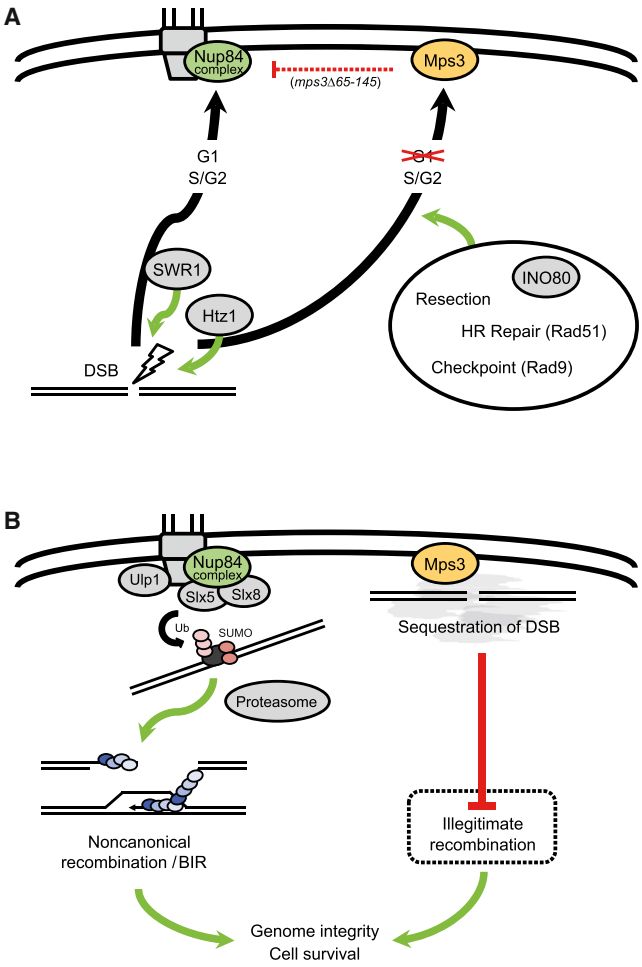

Figure 7. Model of the DSB Relocation and the Outcome

(A) SWR-C and INO80 influence DSB relocation to either Mps3 or pores, as described in the Results. SWR-C incorporated Htz1 (H2A.Z) is essential throughout the cell cycle. Outside of G1, DSBs can bind Mps3 in an INO80- and Rad51-dependent manner independent of pore integrity.

(B) DSB binding to nuclear pores and Mps3 suppresses uSCR, a hallmark of the illegitimate recombination.

nuclear pores with the use of three independent assays. Collectively, they show that the loss of Mps3 affects damage binding at pores, but the loss of pore binding does not impair association with Mps3. This means that either Mps3 acts on pore organization in a subtle manner that ablates the DSB interaction site or there is a necessary, but very transient, interaction of irreparable breaks with Mps3 prior to binding the pore. This latter is unlikely, given that the remodeler INO80 is selectively required for break association with Mps3 and not nuclear pores. Indeed, our final insight into DSB position stems from the relationship of chromatin remodelers to the subnuclear positioning of damage, as depicted in the model in Figure 7.

DSB recruitment to nuclear pores in G1 phase depends on SWR-C activity. Because there is neither resection nor available homology from the replicated sister in G1-phase cells, the preferred pathway of repair in G1 phase is NHEJ. Consistently, previous work has shown that SWR-C is required both for efficient Ku80 recruitment to an induced DSB and for optimal error-free NHEJ (van Attikum et al., 2007). DSB-pore interactions may be stabilized by the affinity of yKu for the pore basket components Mlp1 and Mlp2 (Galy et al., 2000). On the other hand, Arp6 binding to pores is independent of Mlp1 and Mlp2 in G1 phase and is dependent on them in S phase (Yoshida et al., 2010). This may suggest that there is more than one anchorage site for DSBs at pores in G1-phase cells. Pore binding was also implicated in NHEJ-dependent repair of subtelomeric DSBs (Therizols et al., 2006). Finally, and in contrast to *swr1*Δ, the INO80-deficient mutant *arp8*Δ did not affect break recruitment to pores in G1, nor did it alter rates of error-free NHEJ (van Attikum et al., 2007).

In S-phase cells, on the other hand, sister chromatid recombination (SCR) becomes the preferred mechanism of DSB repair (González-Barrera et al., 2003; Kadyk and Hartwell, 1992). Although equal SCR is difficult to monitor, unequal exchange (uSCR) can be readily scored. Spontaneous uSCR rates were unaffected in the *nup120*Δ mutant, whereas rates increased in *mps3*Δ*65-145* (Figure 6). Given that DSB-Mps3 binding is intact in the *nup120*Δ mutant, Mps3 most likely serves as a repressor of uSCR. This is consistent with previous reports of enhanced recombination between telomeres in *mps3*Δ*N* mutants (Schober et al., 2009). Whether Mps3 acts simply by sequestration of the free end or by helping to load Mre11 (González-Barrera et al., 2003) and/or cohesin (Cortés-Ledesma and Aguilera, 2006) is unknown. Consistent with our findings, previous work showed the SWR-C-deficient *arp6* mutant has an increased level of spontaneous uSCR in this same assay (Kawashima et al., 2007).

In an assay for ectopic HR, we found that loss of INO80 function (*arp8*Δ) decreased efficiency, whereas *swr1* deletion increased the rate of DSB-induced HR (Figure 6). Collectively, these results argue for a recombination-repressive role for Mps3, which is consistent with previous observations on telomere-telomere exchange and the likelihood of DNA-DNA interactions detected in a chromosome conformation capture technology (Oza et al., 2009; Schober et al., 2009). Given that we score a delayed but intact DSB-pore interaction in INO80-deficient strains (Figure 2), we propose that nuclear pore association normally does not repress recombination. However, if Mps3 binding is ablated, then S-phase association with nuclear pores may compensate, as supported by the additive effects of the double *nup120 mps3*Δ*65-145* mutant on uSCR. Consistent with this, spontaneous Rad52 foci were found to be more mobile in *arp8* and in *swr1* mutants, which might favor ectopic repair over SCR (data not shown; Dion et al., 2013). We speculate that the role of the nuclear pore in S-phase DSB repair may reflect SUMO- and/or ubiquitin metabolism because of the nuclear pore-associated SUMO protease Ulp1 and the SUMO-dependent ubiquitin ligase Slx5-Slx8 (Nagai et al., 2008; Zhao et al., 2004). Strains mutant for the Nup84 complex (Nup84, Nup120, and Nup133) are hypersensitive to DNA-damaging agents, synthetic lethal with mutations that impair HR, and accumulate spontaneous damage foci containing Rad52 (Nagai et al., 2008; Palancade et al., 2007).

How do remodelers affect DSB binding site choice? The catalytic effects of the INO80 complex under conditions of DNA

damage are well documented and include nucleosome eviction, enhanced resection, and enhanced subdiffusive mobility (reviewed in Seeber et al., 2013b). It is likely that INO80 acts on the substrate itself, generating 3′ overhang without remaining bound to tether the break to Mps3, given that Ino80, Arp5, or Arp8, when fused to LexA, could not shift a tagged locus to the nuclear periphery (Figure S4). The contribution of SWR-C and Htz1 to DSB relocation and repair may instead reflect their binding at the break site. A role for SWR-C and Htz1 in DSB repair appears to be conserved in mammals, given that the Swr1 homolog p400 ATPase and H2A.Z play critical roles in Rad51-mediated repair (Courilleau et al., 2012; Xu et al., 2012). The striking deposition of H2A.Z at laser-induced damage in mammalian cells correlates with an open conformation of chromatin at DSBs and the loading of the Brca1 complex (Xu et al., 2012). Additionally, H2A.Z exchange appears to restrict formation of ssDNA and favor loading of the Ku70/Ku80 complex. We propose that, in yeast, the equivalent phenomenon is break sequestration by Mps3, which is indeed Htz1 dependent. Intriguingly, SWR-C favors Ku loading in yeast (van Attikum et al., 2007), just as its homolog, SRCAP, does in mammalian cells (Xu et al., 2012), which may suppress recombination by sequestration and thus favor NHEJ. Given that remodelers show conserved functions in surviving DNA damage, it is most likely that a spatial segregation of repair functions, such as that shown here, is a conserved aspect of the cell's arsenal of defense against genomic insult.

EXPERIMENTAL PROCEDURES

Plasmids, Yeast Strains, and Yeast Techniques

Yeast strains used in this study are described in Table S1. Conditions for DSB induction and relocalization were previously described (Nagai et al., 2008), and cell culture and synchronization conditions are described in the Supplemental Information.

Microscopy and Movie Analysis

Fluorescence microscopy and quantification was performed according to Meister et al. (2010). For specific details, see the Supplemental Information. Movie analysis and other parameters are available in Table S2.

Statistical Analyses and Cutting Efficiency

To determine zone enrichment, we applied a χ^2 test comparing zone 1 to a random distribution (degree of freedom = 2, confidence limit = 95%). p values are listed in Table S3. To compare the perinuclear enrichment of two different strains, we used a proportional analysis with a confidence limit of 95%. The error bars of all mean squared displacement (MSD) plots and ChIP experiments represent the SEM. The uSCR results were compared with a Student's t test. The efficiency of DSB induction was determined by quantitative PCR with TaqMan probes as previously described (van Attikum et al., 2007). The cutting efficiencies are available in Table S3.

Chromatin Immunoprecipitation

ChIP was carried out as previously described (Yoshida et al., 2010) with modifications described in the Supplemental Information.

Assay for Spontaneous Unequal SCR

uSCR was previously described (Ui et al., 2007) with the generation of functional *ADE3* by reciprocal recombination or gene conversion. Ade3 participates in histidine prototrophy, and thus recombination frequency was monitored by scoring viable colonies on SC-His. After growth at 30°C overnight, cells were collected by centrifugation, washed once, counted, and appropriately diluted onto either yeast extract, bactopeptone, adenine, dextrose (YPAD; 10^3 cells) in order to determine cell viability or SC-His (10^6 cells). Colonies were scored after 3–4 days at 30°C.

SUPPLEMENTAL INFORMATION

Supplemental Information includes Supplemental Experimental Procedures, five figures, and three tables and can be found with this article online at http://dx.doi.org/10.1016/j.molcel.2014.06.027.

ACKNOWLEDGMENTS

We thank Y. Orihara for help in ChIP experiments, J.E. Haber and M. Seki for yeast strains, S.L. Jaspersen, C. Wu, and K. Mizuta for plasmids, and the Friedrich Miescher Institute Microscopy Facility for technical help. C.H. thanks the Marie Curie International program and JSPS Research Abroad program for fellowships. S.M.G. thanks the Novartis Research Foundation, the Swiss National Science Foundation Sinergia grant, NCCR Frontiers in Genetics, and the Human Frontier Science Program (RGP0017) for support, and M.H. is supported by the Grant-in-Aid for Scientific Research on Innovative Areas.

Received: January 22, 2014
Revised: May 5, 2014
Accepted: June 17, 2014
Published: July 24, 2014

REFERENCES

Aguilera, A., and García-Muse, T. (2013). Causes of genome instability. Annu. Rev. Genet. *47*, 1–32.

Bennett, G., Papamichos-Chronakis, M., and Peterson, C.L. (2013). DNA repair choice defines a common pathway for recruitment of chromatin regulators. Nat Commun *4*, 2084–2092.

Chapman, J.R., Taylor, M.R., and Boulton, S.J. (2012). Playing the end game: DNA double-strand break repair pathway choice. Mol. Cell *47*, 497–510.

Chen, X., Cui, D., Papusha, A., Zhang, X., Chu, C.D., Tang, J., Chen, K., Pan, X., and Ira, G. (2012). The Fun30 nucleosome remodeller promotes resection of DNA double-strand break ends. Nature *489*, 576–580.

Cortés-Ledesma, F., and Aguilera, A. (2006). Double-strand breaks arising by replication through a nick are repaired by cohesin-dependent sister-chromatid exchange. EMBO Rep. *7*, 919–926.

Costelloe, T., Louge, R., Tomimatsu, N., Mukherjee, B., Martini, E., Khadaroo, B., Dubois, K., Wiegant, W.W., Thierry, A., Burma, S., et al. (2012). The yeast Fun30 and human SMARCAD1 chromatin remodellers promote DNA end resection. Nature *489*, 581–584.

Courilleau, C., Chailleux, C., Jauneau, A., Grimal, F., Briois, S., Boutet-Robinet, E., Boudsocq, F., Trouche, D., and Canitrot, Y. (2012). The chromatin remodeler p400 ATPase facilitates Rad51-mediated repair of DNA double-strand breaks. J. Cell Biol. *199*, 1067–1081.

Dilworth, D.J., Tackett, A.J., Rogers, R.S., Yi, E.C., Christmas, R.H., Smith, J.J., Siegel, A.F., Chait, B.T., Wozniak, R.W., and Aitchison, J.D. (2005). The mobile nucleoporin Nup2p and chromatin-bound Prp20p function in endogenous NPC-mediated transcriptional control. J. Cell Biol. *171*, 955–965.

Dion, V., Kalck, V., Horigome, C., Towbin, B.D., and Gasser, S.M. (2012). Increased mobility of double-strand breaks requires Mec1, Rad9 and the homologous recombination machinery. Nat. Cell Biol. *14*, 502–509.

Dion, V., Kalck, V., Seeber, A., Schleker, T., and Gasser, S.M. (2013). Cohesin and the nucleolus constrain the mobility of spontaneous repair foci. EMBO Rep. *14*, 984–991.

Doye, V., Wepf, R., and Hurt, E.C. (1994). A novel nuclear pore protein Nup133p with distinct roles in poly(A)+ RNA transport and nuclear pore distribution. EMBO J. *13*, 6062–6075.

Fernandez-Martinez, J., Phillips, J., Sekedat, M.D., Diaz-Avalos, R., Velazquez-Muriel, J., Franke, J.D., Williams, R., Stokes, D.L., Chait, B.T.,

Sali, A., and Rout, M.P. (2012). Structure-function mapping of a heptameric module in the nuclear pore complex. J. Cell Biol. *196*, 419–434.

Galy, V., Olivo-Marin, J.C., Scherthan, H., Doye, V., Rascalou, N., and Nehrbass, U. (2000). Nuclear pore complexes in the organization of silent telomeric chromatin. Nature *403*, 108–112.

Gardner, J.M., Smoyer, C.J., Stensrud, E.S., Alexander, R., Gogol, M., Wiegraebe, W., and Jaspersen, S.L. (2011). Targeting of the SUN protein Mps3 to the inner nuclear membrane by the histone variant H2A.Z. J. Cell Biol. *193*, 489–507.

González-Barrera, S., Cortés-Ledesma, F., Wellinger, R.E., and Aguilera, A. (2003). Equal sister chromatid exchange is a major mechanism of double-strand break repair in yeast. Mol. Cell *11*, 1661–1671.

Horigome, C., Okada, T., Shimazu, K., Gasser, S.M., and Mizuta, K. (2011). Ribosome biogenesis factors bind a nuclear envelope SUN domain protein to cluster yeast telomeres. EMBO J. *30*, 3799–3811.

Ira, G., Pellicioli, A., Balijja, A., Wang, X., Fiorani, S., Carotenuto, W., Liberi, G., Bressan, D., Wan, L., Hollingsworth, N.M., et al. (2004). DNA end resection, homologous recombination and DNA damage checkpoint activation require CDK1. Nature *431*, 1011–1017.

Jackson, S.P., and Bartek, J. (2009). The DNA-damage response in human biology and disease. Nature *461*, 1071–1078.

Kadyk, L.C., and Hartwell, L.H. (1992). Sister chromatids are preferred over homologs as substrates for recombinational repair in Saccharomyces cerevisiae. Genetics *132*, 387–402.

Kadyk, L.C., and Hartwell, L.H. (1993). Replication-dependent sister chromatid recombination in rad1 mutants of Saccharomyces cerevisiae. Genetics *133*, 469–487.

Kalocsay, M., Hiller, N.J., and Jentsch, S. (2009). Chromosome-wide Rad51 spreading and SUMO-H2A.Z-dependent chromosome fixation in response to a persistent DNA double-strand break. Mol. Cell *33*, 335–343.

Kawashima, S., Ogiwara, H., Tada, S., Harata, M., Wintersberger, U., Enomoto, T., and Seki, M. (2007). The INO80 complex is required for damage-induced recombination. Biochem. Biophys. Res. Commun. *355*, 835–841.

Khadaroo, B., Teixeira, M.T., Luciano, P., Eckert-Boulet, N., Germann, S.M., Simon, M.N., Gallina, I., Abdallah, P., Gilson, E., Géli, V., and Lisby, M. (2009). The DNA damage response at eroded telomeres and tethering to the nuclear pore complex. Nat. Cell Biol. *11*, 980–987.

Kobor, M.S., Venkatasubrahmanyam, S., Meneghini, M.D., Gin, J.W., Jennings, J.L., Link, A.J., Madhani, H.D., and Rine, J. (2004). A protein complex containing the conserved Swi2/Snf2-related ATPase Swr1p deposits histone variant H2A.Z into euchromatin. PLoS Biol. *2*, E131.

Krogan, N.J., Keogh, M.C., Datta, N., Sawa, C., Ryan, O.W., Ding, H., Haw, R.A., Pootoolal, J., Tong, A., Canadien, V., et al. (2003). A Snf2 family ATPase complex required for recruitment of the histone H2A variant Htz1. Mol. Cell *12*, 1565–1576.

Light, W.H., Brickner, D.G., Brand, V.R., and Brickner, J.H. (2010). Interaction of a DNA zip code with the nuclear pore complex promotes H2A.Z incorporation and INO1 transcriptional memory. Mol. Cell *40*, 112–125.

Loeillet, S., Palancade, B., Cartron, M., Thierry, A., Richard, G.F., Dujon, B., Doye, V., and Nicolas, A. (2005). Genetic network interactions among replication, repair and nuclear pore deficiencies in yeast. DNA Repair (Amst.) *4*, 459–468.

Luk, E., Ranjan, A., Fitzgerald, P.C., Mizuguchi, G., Huang, Y., Wei, D., and Wu, C. (2010). Stepwise histone replacement by SWR1 requires dual activation with histone H2A.Z and canonical nucleosome. Cell *143*, 725–736.

Meister, P., Gehlen, L.R., Varela, E., Kalck, V., and Gasser, S.M. (2010). Visualizing yeast chromosomes and nuclear architecture. Methods Enzymol. *470*, 535–567.

Miné-Hattab, J., and Rothstein, R. (2012). Increased chromosome mobility facilitates homology search during recombination. Nat. Cell Biol. *14*, 510–517.

Mizuguchi, G., Shen, X., Landry, J., Wu, W.H., Sen, S., and Wu, C. (2004). ATP-driven exchange of histone H2AZ variant catalyzed by SWR1 chromatin remodeling complex. Science *303*, 343–348.

Nagai, S., Dubrana, K., Tsai-Pflugfelder, M., Davidson, M.B., Roberts, T.M., Brown, G.W., Varela, E., Hediger, F., Gasser, S.M., and Krogan, N.J. (2008). Functional targeting of DNA damage to a nuclear pore-associated SUMO-dependent ubiquitin ligase. Science *322*, 597–602.

Neumann, F.R., Dion, V., Gehlen, L.R., Tsai-Pflugfelder, M., Schmid, R., Taddei, A., and Gasser, S.M. (2012). Targeted INO80 enhances subnuclear chromatin movement and ectopic homologous recombination. Genes Dev. *26*, 369–383.

Oza, P., and Peterson, C.L. (2010). Opening the DNA repair toolbox: localization of DNA double strand breaks to the nuclear periphery. Cell Cycle *9*, 43–49.

Oza, P., Jaspersen, S.L., Miele, A., Dekker, J., and Peterson, C.L. (2009). Mechanisms that regulate localization of a DNA double-strand break to the nuclear periphery. Genes Dev. *23*, 912–927.

Palancade, B., Liu, X., Garcia-Rubio, M., Aguilera, A., Zhao, X., and Doye, V. (2007). Nucleoporins prevent DNA damage accumulation by modulating Ulp1-dependent sumoylation processes. Mol. Biol. Cell *18*, 2912–2923.

Papamichos-Chronakis, M., and Peterson, C.L. (2008). The Ino80 chromatin-remodeling enzyme regulates replisome function and stability. Nat. Struct. Mol. Biol. *15*, 338–345.

Papamichos-Chronakis, M., Krebs, J.E., and Peterson, C.L. (2006). Interplay between Ino80 and Swr1 chromatin remodeling enzymes regulates cell cycle checkpoint adaptation in response to DNA damage. Genes Dev. *20*, 2437–2449.

Papamichos-Chronakis, M., Watanabe, S., Rando, O.J., and Peterson, C.L. (2011). Global regulation of H2A.Z localization by the INO80 chromatin-remodeling enzyme is essential for genome integrity. Cell *144*, 200–213.

Peterson, C.L., and Almouzni, G. (2013). Nucleosome dynamics as modular systems that integrate DNA damage and repair. Cold Spring Harb. Perspect. Biol. *5*, http://dx.doi.org/10.1101/cshperspect.a012658.

Pfeiffer, P., Goedecke, W., and Obe, G. (2000). Mechanisms of DNA double-strand break repair and their potential to induce chromosomal aberrations. Mutagenesis *15*, 289–302.

Price, B.D., and D'Andrea, A.D. (2013). Chromatin remodeling at DNA double-strand breaks. Cell *152*, 1344–1354.

Schober, H., Ferreira, H., Kalck, V., Gehlen, L.R., and Gasser, S.M. (2009). Yeast telomerase and the SUN domain protein Mps3 anchor telomeres and repress subtelomeric recombination. Genes Dev. *23*, 928–938.

Seeber, A., Dion, V., and Gasser, S.M. (2013a). Checkpoint kinases and the INO80 nucleosome remodeling complex enhance global chromatin mobility in response to DNA damage. Genes Dev. *27*, 1999–2008.

Seeber, A., Hauer, M., and Gasser, S.M. (2013b). Nucleosome remodelers in double-strand break repair. Curr. Opin. Genet. Dev. *23*, 174–184.

Shen, X., Mizuguchi, G., Hamiche, A., and Wu, C. (2000). A chromatin remodelling complex involved in transcription and DNA processing. Nature *406*, 541–544.

Shimada, K., Oma, Y., Schleker, T., Kugou, K., Ohta, K., Harata, M., and Gasser, S.M. (2008). Ino80 chromatin remodeling complex promotes recovery of stalled replication forks. Curr. Biol. *18*, 566–575.

Smeenk, G., and van Attikum, H. (2013). The chromatin response to DNA breaks: leaving a mark on genome integrity. Annu. Rev. Biochem. *82*, 55–80.

Taddei, A., Hediger, F., Neumann, F.R., Bauer, C., and Gasser, S.M. (2004). Separation of silencing from perinuclear anchoring functions in yeast Ku80, Sir4 and Esc1 proteins. EMBO J. *23*, 1301–1312.

Therizols, P., Fairhead, C., Cabal, G.G., Genovesio, A., Olivo-Marin, J.C., Dujon, B., and Fabre, E. (2006). Telomere tethering at the nuclear periphery is essential for efficient DNA double strand break repair in subtelomeric region. J. Cell Biol. *172*, 189–199.

Tsukuda, T., Fleming, A.B., Nickoloff, J.A., and Osley, M.A. (2005). Chromatin remodelling at a DNA double-strand break site in Saccharomyces cerevisiae. Nature *438*, 379–383.

Ui, A., Seki, M., Ogiwara, H., Lai, M.S., Yamamoto, K., Tada, S., and Enomoto, T. (2007). Activation of a novel pathway involving Mms1 and Rad59 in sgs1 cells. Biochem. Biophys. Res. Commun. *356*, 1031–1037.

van Attikum, H., Fritsch, O., Hohn, B., and Gasser, S.M. (2004). Recruitment of the INO80 complex by H2A phosphorylation links ATP-dependent chromatin remodeling with DNA double-strand break repair. Cell *119*, 777–788.

van Attikum, H., Fritsch, O., and Gasser, S.M. (2007). Distinct roles for SWR1 and INO80 chromatin remodeling complexes at chromosomal double-strand breaks. EMBO J. *26*, 4113–4125.

Wu, W.H., Alami, S., Luk, E., Wu, C.H., Sen, S., Mizuguchi, G., Wei, D., and Wu, C. (2005). Swc2 is a widely conserved H2AZ-binding module essential for ATP-dependent histone exchange. Nat. Struct. Mol. Biol. *12*, 1064–1071.

Xu, Y., Ayrapetov, M.K., Xu, C., Gursoy-Yuzugullu, O., Hu, Y., and Price, B.D. (2012). Histone H2A.Z controls a critical chromatin remodeling step required for DNA double-strand break repair. Mol. Cell *48*, 723–733.

Yoshida, T., Shimada, K., Oma, Y., Kalck, V., Akimura, K., Taddei, A., Iwahashi, H., Kugou, K., Ohta, K., Gasser, S.M., and Harata, M. (2010). Actin-related protein Arp6 influences H2A.Z-dependent and -independent gene expression and links ribosomal protein genes to nuclear pores. PLoS Genet. *6*, e1000910.

Zhao, X., Wu, C.Y., and Blobel, G. (2004). Mlp-dependent anchorage and stabilization of a desumoylating enzyme is required to prevent clonal lethality. J. Cell Biol. *167*, 605–611.